Inorg. Chem. **2003**, *42*, 8902–8910

On the Origin of the Optical Activity in the d–d Transition Region of Tris-Bidentate Co(III) and Rh(III) Complexes

Francisco E. Jorge,[†,‡] Jochen Autschbach,[†,§] and Tom Ziegler*[,†]

Department of Chemistry, University of Calgary, Calgary, Alberta, Canada, T2N-1N4, Departamento de Fisica, Universidade Federal do Espirito Santo, 29060-900 Vitoria, ES, Brazil, and Department of Chemistry, University at Buffalo, State University of New York, 312 Natural Sciences Complex, Buffalo, New York 14260-3000

Received August 22, 2003

Time-dependent density functional theory (TD-DFT) has been employed to calculate the rotatory strengths in the d–d transition region for various tris-bidentate Co(III) and Rh(III) complexes. Optimized structural parameters are also reported. Our results confirm a previously proposed relationship between the azimuthal distortion of a complex containing saturated tris(diamine) and its optical activity. Formally d–d transitions are forbidden and should not exhibit optical activity. However, it is shown here that the intensity of these bands originates from a coupling of even ligand combination (participating in the e_g type LUMO) and an odd ligand combination (participating in the t_{2g} HOMO). For complexes containing planar unsaturated ligands, the signs of the d–d bands observed from the single-crystal circular and linear dichroisms are in accordance with the TD-DFT predictions. It is shown that by using hypothetical $Co(NH_3)_6^{3+}$ complexes it is possible to estimate the contribution from the azimuthal distortion to the total rotatory strengths of the saturated tris(diamine) complexes. A discussion is also provided of previous theoretical studies and the way in which these investigations rationalized the optical activity.

1. Introduction

The optical activity of transition metal complexes in the region of the d−d absorption bands has been the subject of theoretical and experimental investigations for some time.[1,2] It is known that the rotatory strengths associated with this region are considerably smaller than those usually observed for fully allowed transitions. Much of the theoretical work in this field has been aimed at accounting for the signs and magnitudes of the observed rotations.

Tris-bidentate Co(III) and Cr(III) complexes, Scheme 1, usually give rise to two circular dichroism (CD) bands of opposite sign in the region of the lowest energy. The symmetry of the transition responsible for this absorption bands is $^1T_{1g}$ in effective O_h symmetry, and the two CD bands correspond to the E and A_2 components of the originally $^1T_{1g}$ transition generated when the symmetry of the complex is reduced from O_h to D_3 , see Scheme 2. The simpler theoretical models relate the magnitude of this E−A_2 splitting to an axial distortion of the octahedron along the 3-fold axis of the complex,[1] Scheme 3. On the other hand, signs and magnitudes of the rotatory strengths of the individual bands are usually considered to be the result of the conformational and configuration effects of the rings[1] including the azimuthal distortions of the octahedron, Scheme 4.

Scheme 1. The Δ- and Λ-Configurations of $Co(en)_3^{3+}$

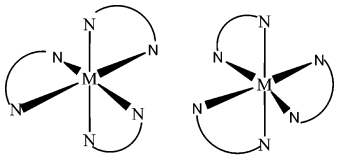

Δ-M(en)$_3^{3+}$ **Λ-M(en)$_3^{3+}$**

Theoretical studies of transition metal complexes have focused almost exclusively on complexes of Co(III) and Cr-(III) with saturated amines. Moffitt[3] reformulated the fundamental electron theory of optical activity proposed by

* Author to whom correspondence should be addressed. E-mail: ziegler@ucalgary.ca.
† University of Calgary.
‡ Universidade Federal do Espirito Santo.
§ University at Buffalo.

(1) Mason, S. F. In *Fundamental aspects and recent developments in optical rotatory dispersion and circular dichroism*; Ciardelli, F., Salvadori, P., Eds.; Heyden and Son Ltd.: London, 1973; Chapter 3.6.
(2) Saito, Y. *Coord. Chem. Rev.* **1974**, *13*, 305 and references therein.
(3) Moffitt, W. *J. Chem. Phys.* **1956**, *25*, 1189.

10.1021/ic034997t CCC: $25.00
Published on Web 11/18/2003

Scheme 2. The Lowest Singlet Excited States for an Octahedral Complex with a d^6 Ground State Configuration, and Their Splitting on Reduction of the Symmetry into D_{3h} and D_3 Point Group Symmetry

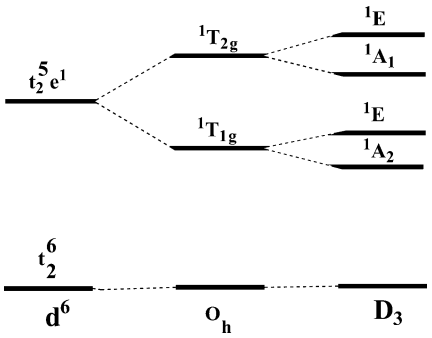

Scheme 3. Polar Distortion of the Octahedron

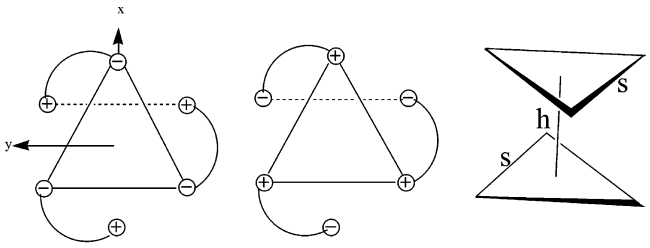

Scheme 4. Azimuthal Distortion of the Octahedron

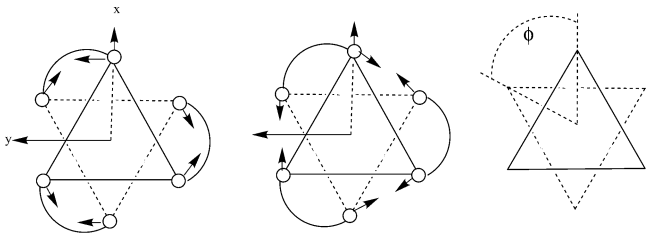

Condon *et al.*[4] into a theory of optical activity based on crystal field theory. An important step forward was taken by Liehr[5] and Karipides,[6] who formulated the theory of optical activity for metal complexes in the language of molecular orbital theory. In fact, many subsequent theoretical developments[7,8] were based on the Liehr model.[5] However other interesting approaches have also appeared, including the independent system perturbation theory that includes static point charge crystal field theory[9]as well as the dynamic coupling method.[10,11] Unfortunately, the formidable complexity[10b] of some of these theories restricts their usage and development to a limited number of specialists.

The models of Karipides and Piper[6] and Mason and Seal[11] seem to correctly predict the spectra of complexes containing saturated diamines and similar ligands, but none of these methods have been able to explain the results reported for planar unsaturated ligands, where the spectrum appears to be affected by π electrons on the ligands.[12]

Recently, there has been an increasing interest in the calculation of optical activity by time-dependent density functional theory (TD-DFT),[13−16] because this approach "combines moderate accuracy with low computational cost and provides a simple intuitive interpretation".[17] The TD-DFT method has been used with success in calculations of excitation energies and transition moments of hydrocarbons, at least for excitations well bellow the ionization limit,[18,19] as well as in calculations of excitation energies of some selected transition metal complexes.[20−26] Recent studies[27,28] of chiral complexes showed that fair agreement between TD-DFT and experimental absorption and CD spectra[28] can be achieved also for large transition metal compounds.

In this work the TD-DFT method is used to evaluate the rotatory strengths (R) and singlet excitation energies (ν) of the d−d transitions of some Co(III) and Rh(III) complexes in gas phase, namely: Λ-Co(en)$_3^{3+}$, Λ-Rh(en)$_3^{3+}$, Λ-Co(pn)$_3^{3+}$, Λ-Rh(pn)$_3^{3+}$, Λ-Co(tn)$_3^{3+}$, Λ-Co(acac)$_3$, Λ-Co(ox)$_3^{3-}$, and Λ-Co(NH$_3$)$_6^{3+}$, where the abbreviations used are en = ethylenediamine, tn = trimethylenediamine, pn = propylenediamine, acac = pentane-2,4-dionato, and ox = oxalate. We will consider distortions of the octahedron to consist of an axial (or polar) displacement which will elongate or compress the octahedron along the 3-fold axis C_3, see Scheme 3, and a radial (or azimuthal) distortion consisting of a twist about the 3-fold axis, see Scheme 4. In accordance with the nomenclature developed by Stiefel and Brown,[29] we will use the parameter s/h (side/height), see

(4) Condon, E. U.; Alter, W.; Eyring, H. *J. Chem. Phys.* **1937**, *5*, 753.
(5) Liehr, A. D. *J. Phys. Chem.* **1964**, *68*, 665.
(6) Karipides, A.; Piper, T. S. *J. Chem. Phys.* **1964**, *40*, 674.
(7) Strickland, R. W.; Richardson, F. S. *Inorg. Chem.* **1973**, *12*, 1025.
(8) Evans, R. S.; Schreiner, A. F.; Hauser, P. J. *Inorg. Chem.* **1974**, *13*, 2185.
(9) Richardson, F. S. *Inorg. Chem.* **1972**, *11*, 2366.
(10) (a) Richardson, F. S. *J. Chem. Phys.* **1971**, *54*, 2453. (b) Kuroda, R.; Saito, Y. Circular dichroism of inorganic complexes: Interpretation and applications. In *Circular Dichroism. Principles and Applications*; Nakanishi, K., Berova, N., Woody, R. W., Eds.; VCH: New York, 1994.
(11) Mason, S. F.; Seal, R. H. *Mol. Phys.* **1976**, *31*, 755.
(12) Moucharafieh, N. C.; Eller, P. G.; Bertrand, J. A.; Royer, D. J. *Inorg. Chem.* 1978, *17*, 1220.
(13) Casida, M. E. Time-dependent density functional response theory for molecules. In *Recent advances in density functional methods*, Vol. 1; Chong, D. P., Ed.; World Scientific: Singapore, 1995.
(14) Gross, E. K. U.; Kohn, W. *Adv. Quantum Chem.* **1990**, *21*, 255.
(15) Gross, E. K. U.; Dobson, J. F.; Petersilka, M. *Top. Curr. Chem.* **1996**, *181*, 81.
(16) Dobson, J. F. Time-dependent density functional theory. In *Electronic density functional theory. Recent progress and new directions*; Dobson, J. F., Vignale, G., Das, M. P., Eds.; Plenum Press: New York, 1998.
(17) Furche, F.; Ahlrichs, R.; Wachsmann, C.; Weber, E.; Sobanski, A.; Vögtle, F.; Grimme, S. *J. Am. Chem. Soc.* **2000**, *122*, 1717.
(18) Bauernschmitt, R.; Ahlrichs, R. *Chem. Phys. Lett.* **1996**, *256*, 454.
(19) Jamorski, C.; Casida, M. E.; Salahub, D. R. *J. Chem. Phys.* **1996**, *104*, 5134.
(20) Solomon, E. I., Lever, A. B. P., Eds. *Inorganic Electronic Structure and Spectroscopy;* Wiley: New York, 1999; Vols. 1 and 2.
(21) Rosa, A.; Baerends, E. J.; van Gisbergen, S. J. A.; van Lenthe, E.; Groeneveld, J. A.; Snijders, N. G. *J. Am. Chem. Soc.* **1999**, *121*, 10356.
(22) Ricciardi, G.; Rosa, A.; Baerends, E. J. *J. Phys. Chem. A* **2001**, *105*, 5242.
(23) Rosa, A.; Ricciardi, G.; Baerends, E. J.; van Gisbergen, S. J. A. *J. Phys. Chem. A* **2001**, *105*, 3311.
(24) Ricciardi, G.; Rosa, A.; van Gisbergen, S. J. A.; Baerends, E. J. *J. Phys. Chem. A* **2000**, *104*, 635−643.
(25) van Gisbergen, S. J. A.; Groeneveld, J. A.; Rosa, A.; Snijders, J. G.; Baerends, E. J. *J. Phys. Chem. A* **1999**, *103*, 6835.
(26) (a) Ziegler, T. *J. Chem. Soc., Dalton Trans.* **2002**, 642. (b) Patchkovskii, S.; Ziegler, T. *J. Chem. Phys.* **2002**, *116*, 7806
(27) Gorelsky, S. I.; Lever, A. B. P. *J. Organomet. Chem.* **2001**, *635*, 187.
(28) Autschbach, J.; Jorge, F. E.; Ziegler, T. *Inorg. Chem.* **2003**, *42*, 2867.
(29) Stiefel, E. I.; Brown, G. F. *Inorg. Chem.* **1972**, *11*, 434.

Scheme 3, as a measure for the polar displacement and Φ, see Scheme 4, as a parameter for the radial (or azimuthal) distortion. We recall that for an octahedron $s/h = 1.22$ and $\Phi = 60°$. The reason for considering these is that, to first order, s/h and Φ are associated with the $E-A_2$ energy separation and the rotatory strength, respectively. Our results for ν, R, s/h, and Φ are compared with the corresponding theoretical and experimental values available in the literature.[8,11,30−36] For some complexes, electric transition dipole moments (TDMs) are also calculated.

Section 2 presents the computational details whereas the computational results are presented and discussed in section 3. We give, finally, in section 4 some concluding remarks.

2. Computational Details

Singlet excitation energies and rotatory strengths of the d−d transitions have been calculated with a modified CD version of the Amsterdan Density Functional (ADF) program.[37−39] The CD version by Autschbach[40−42] *et al*. is an extension of the TDDFT module in ADF developed by van Gisbergen, Baerends, *et al*.[43−45] within the adiabatic LDA approximation. A triple-ζ polarized (TZP) Slater basis set (IV) from the ADF database was employed in all calculations. Rotatory strengths were evaluated by the dipole-length formula. However, it has recently been shown[28] that the dipole-velocity formula affords quite similar results for $Co(en)_3^{3+}$.

The Vosko−Wilk−Nusair[46] local density approximation (LDA) with Becke88−Perdew86 (BP86) gradient corrections[47,48] has been employed in all CD calculations. The CD calculations are based on optimized geometries (VWN functional, TZP basis set) except for the $Co(tn)_3^{3+}$ complex where the experimental geometry[32] for the crystals used to measure the spectrum is considerably distorted by counterions. In those cases where the rotatory strengths have been obtained for the Δ-configuration, the experimental data for the Λ-configuration are reported in Table 1 with the opposite signs. The ADFview code was employed to visualize some of the molecular orbitals.

(30) Judkins, R. R.; Royer, D. J. *Inorg. Chem.* **1974**, *13*, 945.
(31) Nakatsu, K. *Bull. Chem. Soc. Jpn.* **1962**, *35*, 832.
(32) Nagao, R.; Marumo, F.; Saito, Y. *Acta Crystallogr*. **1973**, *B29*, 2438.
(33) Kuroda, R.; Saito, Y. *Acta Crystallogr.* **1974**, *B30*, 2126.
(34) Kruger, G. J.; Reynhardt, E. C. *Acta Crystallogr., Sect. B* **1974**, *30*, 822.
(35) Butler, K. R.; Snow, M. R. *J. Chem. Soc. A* **1971**, 565.
(36) Kuroda, R.; Saito, Y. *Bull. Chem. Soc. Jpn.* **1976**, *49*, 433.
(37) Fonseca Guerra, C.; Visser, O.; Snijders, J. G.; te Velde, G.; Baerends, E. J. Parallelisation of the Amsterdam Density Functional program Program. In *Methods and Techniques for Computational Chemistry*; STEF: Cagliari, 1995.
(38) te Velde, G.; Bickelhaupt, F. M.; Baerends, E. J.; van Gisbergen, S. J. A.; Fonseca Guerra, C.; Snijders, J. G.; Ziegler, T. *J. Comput. Chem.* **2001**, *22*, 931.
(39) "Amsterdam Density Functional program", Theoretical Chemistry, Vrije Universiteit, Amsterdam, URL: http://www.scm.com (accessed Nov 2002).
(40) Autschbach, J.; Ziegler, T.; van Gisbergen, S. J. A.; Baerends, E. J. *J. Chem. Phys.* **2002**, *116*, 6930−6940.
(41) Autschbach, J.; Ziegler, T. *J. Chem. Phys.* **2002**, *116*, 891.
(42) Autschbach, J.; Ziegler, T.; Patchkovskii, S.; van Gisbergen, S. J. A.; Baerends, E. J. *J. Chem. Phys.* **2002**, *117*, 581−592.
(43) van Gisbergen, S. J. A.; Snijders, J. G.; Baerends, E. J. *J. Chem. Phys.* **1995**, *103*, 9347.
(44) van Gisbergen, S. J. A.; Snijders, J. G.; Baerends, E. J. *Comput. Phys. Commun.* **1999**, *118*, 119.
(45) van Gisbergen, S. J. A.; Fonseca-Guerra, C.; Baerends, E. J. *J. Comput. Chem.* **2000**, *21*, 1511−1523.
(46) Vosko, S. H.; Wilk, L.; Nusair, M. *Can. J. Phys.* **1980**, *58*, 1200.
(47) Becke, A. D. *Phys. Rev. A* **1988**, *38*, 3098.
(48) Perdew, J. P. *Phys. Rev. B* **1986**, *33*, 8822.

3. Results and Discussion

The relevant spectral and structural information concerning the transition metal complexes studied here is summarized in Table 1. This table displays the rotatory strengths (R in 10^{-40} cgs units), the excitation energies (ν in 10^{-3} cm^{-1}), the $E-A_2$ splitting ($\nu_E - \nu_{A2}$ in 10^{-3} cm^{-1}) of the d−d transition bands, and the polar (Scheme 3) and azimuthal (Scheme 4) distortions s/h and Φ (in deg), respectively, for a number of d^6 metal complexes in the gas phase. The complexes include Λ-$Co(en)_3^{3+}$, Λ-$Rh(en)_3^{3+}$, Λ-$Co(pn)_3^{3+}$, Λ-$Rh(pn)_3^{3+}$, Λ-$Co(tn)_3^{3+}$, Λ-$Co(acac)_3$, and Λ-$Co(ox)_3^{3-}$. For the diamine complexes both the *lel* (the C−C or C−C−C bond of each chelate ring is parallel, or nearly so, to the C_3-axis) and *ob* (the C−C or C−C−C bond of each chelate ring is obliquely inclined with respect to the the C_3-axis) ligand configurations were considered, Scheme 5. Thus, we have carried out calculations on complexes in which all three ligands were of *lel* or *ob* conformation. We refer to these two configurations as $(lel)^3$ and $(ob)^3$. The spectral properties calculated with the TD-DFT method are compared to other theoretical[8,11] (configuration Λ) and experimental[36] (configuration Λ/Δ) results available in the literature. Polar and azimuthal distortions are also reported for the known experimental structures.[31−35]

Complexes Containing Saturated Tris(diamine). As mentioned before, tris(diamine) complexes usually exhibit two CD bands with opposite signs in the first absorption region ($^1A_{1g} \rightarrow {}^1T_{1g}$), Scheme 2. The two bands correspond to the E and A_2 components of O_h parentage in the D_3 environment. The splittings and signs of the two CD bands in the d−d transition region have been related by Judkins and Royer[30] and others[9,11,29,30] to the polar (s/h of Scheme 3) and azimuthal (Φ of Scheme 4) distortions[29] in a model based on observations as well as ligand field arguments. We shall discuss the justification for this model later. For now we present its predictions in Table 2.

Table 1 reveals that the TD-DFT estimates for the signs of the rotatory strengths and the $\nu_E - \nu_{A2}$ splittings are in agreement with the predictions of Table 2 based on the s/h and Φ values used for the Co(III) and Rh(III) complexes. The only exception is for the $(ob)^3$ Λ-$Co(tn)_3^{3+}$ isomer where the calculated sign for $\nu_E - \nu_{A2}$ is the opposite of what one (Table 2) would predict from the optimized s/h value.

It follows further from the TD-DFT results in Table 1 that $|R(E)|$ is larger than $|R(A_2)|$. The only exception to this rule is the $(lel)^3$ Λ-$Rh(en)_3^{3+}$ isomer. Also, for Λ-$Co(en)_3^{3+}$, Λ-$Rh(en)_3^{3+}$, and Λ-$Rh(pn)_3^{3+}$ complexes, the $|\nu_E - \nu_{A2}|$ values for the $(ob)^3$ conformations are smaller than those with *lel* conformations, whereas for Λ-$Co(pn)_3^{3+}$ and Λ-$Co(tn)_3^{3+}$ the opposite occurs.

For $(lel)^3$-Λ-$[Co(en)_3^{3+}]Br_3 \cdot H_2O$ the dynamic-coupling model[11] affords values for $R(E)$ and $R(A_2)$ of +63.8 and −59.8, respectively, in excellent agreement with the experimental estimates of +59.9 (E) and −55.7 (A_2) from solid-state CD spectra.[36] All these values are larger by a factor of 2, Table 1, than those obtained in the present TD-DFT study. It should be mentioned that much smaller experimental

Table 1. Circular Dichroism and Structural Parameters of Co(III) and Rh(III) Tris-Bidentate Complexes in the Gas Phase

complex	band	R (10^{-40} cgs)	ν (10^3 cm^{-1})	$\nu_E - \nu_{A2}$ (10^3 cm^{-1})	s/h	Φ (deg)
Λ-Co(en)$_3^{3+}$	E	+28.9[a]	26.982[a]	−0.281[a]	1.27[a]	53.7[a]
(*lel*)^3		+63.8[d]				
		+59.9[e] (exp)	20.76[e,o] (exp)	−0.23[e] (exp)	1.25[f] (exp)	56.8[f] (exp)
	A_2	−25.0[a]	27.263[a]			
		−59.8[d]				
		−55.7[e] (exp)	20.99[e,o] (exp)			
Λ-Co(en)$_3^{3+}$	E	+17.5[b]	27.015[b]	−0.220[b]	1.32[b]	55.4[b]
(*ob*)^3	A_2	−12.2[b]	27.235[b]			
Λ-Rh(en)$_3^{3+}$	E	+40.7[a]	33.223[a]	−0.699[a]	1.37[a]	52.1[a]
(*lel*)^3	A_2	−43.4[a]	33.922[a]			
Λ-Rh(en)$_3^{3+}$	E	+36.5[b]	33.239[b]	−0.412[b]	1.41[b]	53.3[b]
(*ob*)^3	A_2	−29.9[b]	33.651[b]			
Λ-Co(pn)$_3^{3+}$	E	+17.2[a]	27.068[a]	−0.360[a]	1.27[a]	52.1[a]
(*lel*)^3		+65.1[d]				
		+38.1[e] (exp)	20.45[e,o] (exp)	−0.38[e] (exp)	1.30[g] (exp)	54.2[g] (exp)
	A	−14.3[a]	27.429[a]			
		−61.3[d]				
		−36.6[e] (exp)	20.83[e,o] (exp)			
Λ-Co(pn)$_3^{3+}$	E	+11.6[b]	27.111[b]	−0.452[b]	1.37[b]	55.2[b]
(*ob*)^3	A	−2.1[b]	27.563[b]			
Λ-Rh(pn)$_3^{3+}$	E	+34.2[a]	33.393[a]	−0.591[a]	1.38[a]	51.4[a]
(*lel*)^3	A	−32.4[a]	33.985[a]			
Λ-Rh(pn)$_3^{3+}$	E	+37.2[b]	33.451[b]	−0.381[b]	1.42[b]	52.9[b]
(*ob*)^3	A	−23.6[b]	33.832[b]			
Λ-Co(tn)$_3^{3+}$	E	−10.6[h]	25.690[h]	−0.260[h]	1.22[h]	61.5[h]
(*lel*)^3		−10.3[d]				
		−10.5[c] (exp)	20.683[c] (exp)	+1.51[c] (exp)		
	A	+8.2[h]	25.950[h]			
Λ-Co(tn)$_3^{3+}$	E	+10.0[b]	26.567[b]	+0.246[b]	1.25[b]	59.6[b]
(*ob*)^3	A	−3.4[b]	26.321[b]			
Λ-Co(acac)$_3$	E	+25.1[j]	21.732[j]	+0.714[j]	1.12[j]	69.3[j]
		+19.6[c] (exp)	17.575[c] (exp)	+1.67[c] (exp)	1.21[c] (exp)	54[c] (exp)
	A_2	−23.4[j]	21.018[j]		1.15[k] (exp)	67.3[k] (exp)
		−7.7[c] (exp)	15.910[c] (exp)			
Λ-Co(ox)$_3^{3-}$	E	+33.7[j]	20.376[j]	−0.330[j]	1.29[j]	56.2[j]
	A_2	−33.8[j]	20.706[j]		1.30[l] (exp)	54.1[l] (exp)

[a] This work ((*lel*)^3 conformation). [b] This work ((*ob*)^3 conformation). [c] Reference 30. [d] Reference 11. [e] Reference 36. [f] Reference 31. [g] Reference 33. [h] Calculated in this work using the experimental geometry ref 32. [i] Reference 32. [j] This work. [k] Reference 34. [l] Reference 35. [m] Using R(E) from ref 30 based on single-crystal CD spectrum of species from ref 32 and R(T1) from Table 3 of ref 11. [n] The abbreviations employed are en = ethylenediamine, tn = trimethylenediamine, pn = 1,2-diamine propane, acac = 2,4 pentanedionate, ox = oxalate. [o] Peak positions of the E and A_2 bands.

Scheme 5. The λ and δ Ligand Conformations

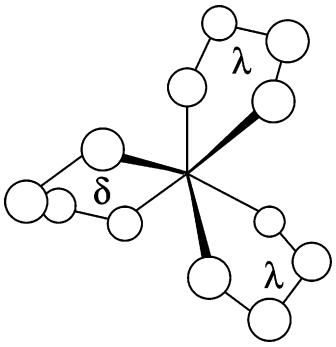

Table 2. Four Structural Varieties I−IV of a Tris(diamine) Complex, as Characterized by s/h and Φ, and the Relationship between Their Geometry and Optical Activity

	E	A_2	$\nu_E - \nu_{A2}$	s/h	Φ
I	>0	<0	<0	>1.22	<60°
II	>0	<0	>0	<1.22	<60°
III	<0	>0	>0	<1.22	>60°
IV	<0	>0	<0	>1.22	>60°

values of −6.2 (A_2) and 10.7 (E), respectively, have been reported by Judkins and Royer[30] from a Gaussian resolution of the CD spectra in solution. However, this procedure is not considered as accurate as single-crystal spectroscopy. The actual calculated excitation energies for Co(en)$_3^{3+}$ are too high by 6000 cm^{-1} or 0.75 eV. Similar errors are seen for the other 3d cobalt systems. It is in general found[26a] that the crystal field splitting is overestimated by approximate DFT for complexes containing metals of the first transition series. The deviation stems from the so-called self-interaction error[26b] which results in a too low energy of the d-orbitals leading to a too large interaction with the ligand orbitals and consequently to an overestimation of the crystal field splitting. The structural parameters optimized by DFT for (*lel*)^3-Λ-Co(en)$_3^{3+}$ are in good agreement with those determined from the crystal structure of Λ-[Co(en)$_3^{3+}$]Br$_3$·H$_2$O.[31] For Λ-Rh(en)$_3^{3+}$ we find a better agreement between the positions of the d−d bands determined experimentally[49] (31.500 cm^{-1}) and computationally (33.400 cm^{-1}), Table 1. The crystal field is generally larger for the second and third row transition metals where the self-interaction error is smaller for the more diffuse 4d and 5d orbitals.[26a] The CD spectrum for Rh(en)$_3^{3+}$ has not been resolved experimentally into its R(A_2) and R(E) components. We find from our calculations that the two components are of the same sign but a factor of 1.5 larger for Rh(III) compared to Co-

(49) McCaffery, A. J.; Mason, S. F.; Ballard, R. E. *J. Chem. Soc.* **1965**, 2883.

(III). This is consistent with the observation of $\Delta\epsilon$ of 23.7 cm^{-1} M^{-1} and 34.6 cm^{-1} M^{-1} for Co(III) and Rh(III), respectively, where $\Delta\epsilon$ is the difference in the extinction coefficients for right and left polarized light at the d−d band center.

In the case of the tris(propylenediamine) complex $(lel)^3$-Λ-$Co(pn)_3^{3+}$ we find again that the rotatory strengths due to TD-DFT of 17.2 (E) and −14.3 (A_2) are about half the size of the experimentally observed component given by 38.1 (E) and −36.6 (A_2), respectively, Table 1. On the other hand, the estimates from the dynamic-coupling model[11] are too large by a factor of 2.

The tris(trimethylenediamine) complex $(lel)^3$-Λ-$Co(tn)_3^{3+}$ is of special interest because the experimental structure[32] used in our calculation (see Computational Details) has a Φ parameter of 61.5°. It should thus according to Table 2 have signs for R(E) and $R(A_2)$ that are opposite to those of the en- and pn-complexes for which both experimental and theoretical Φ parameter are less than 60°, Table 1. We find indeed that our TD-DFT method affords a change in sign with $R(E) = -10.6$ and $R(A_2) = 8.2$. The TD-DFT results are further in good agreement with experiment, −10.5(E) and 10.3 (A_2), as well as results from the dynamic-coupling model:[11] −10.3 (E), 10.1 (A_2).

Complexes Containing Planar Unsaturated Ligands. The assignments of the E and A_2 bands for Λ-$Co(ox)_3^{3-}$ and Λ-$Co(acac)_3$ have been made from single-crystal CD[49] and linear dichroism (LD)[12] spectra, respectively. Moucharafieh *et al.*[12] concluded from their LD investigation on Λ-$Co(acac)_3$ that the E−A_2 separation is greater than 400 cm^{-1} (∼800 cm^{-1}). They assign the lower (negative) CD-band to the $^1A_1 \rightarrow {}^1A_2$ transition and the higher energy (positive) CD-band to the $^1A_1 \rightarrow {}^1E$ transition, in agreement with previous investigations[30,50] and the current set of TD-DFT calculations on Λ-$Co(acac)_3$, Table 1. Thus, the estimated experimental rotatory strengths[30] for the d−d transitions in Λ-$Co(acac)_3$ are 19.6 (E) and −7.7 (A_2) compared to the TD-DFT values of 25.1 (E) and −23.4 (A_2), Table 1.

The single-crystal CD[49] spectra of Λ-$Co(ox)_3^{3-}$ reveals a $^1A_1 \rightarrow {}^1E$ transition with a positive sign for R(E), in agreement with our TD-DFT calculations, Table 1. Unfortunately it was not possible from the experimental CD[49] spectra to locate the $^1A_1 \rightarrow {}^1A_2$ component of the d−d transition. McCaffery[49] et al. assumed that the two transitions are close in energy and that the E-band with a larger rotatory strength completely hides the A_2-component. This assumption is supported by the small separation observed in the LD spectra for the corresponding $Cr(ox)_3^{3+}$ complex.[12] On the other hand, our results for the Λ-$Co(ox)_3^{3-}$ system show that $R(A_2)$ is slightly larger than R(E), and that the E−A_2 shift has the same magnitude as in other systems such as Λ-$Co(en)_3^{3+}$ and Λ-$Co(pn)_3^{3+}$, for which a resolution of both bands has been possible.

Both optimized geometries and experimental crystal structures[34,35] indicate that $Co(acac)_3$ as the first and only system discussed here has an "elongated" polar coordinate

Scheme 6. Numbering Scheme for Ligands in $M(NH_3)_6^{3+}$

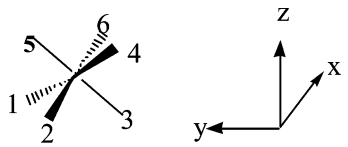

Scheme 7. HOMOs and LUMOs for $M(NH_3)_6^{3+}$ with a d^6 Electron Count

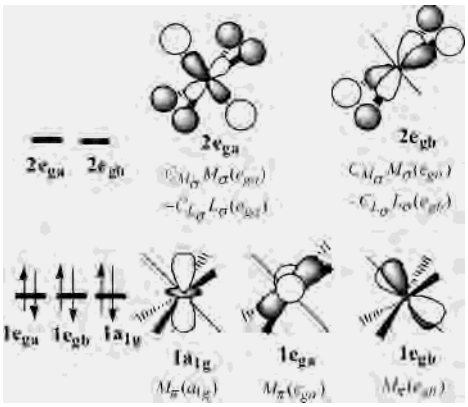

with $s/h < 1.22$, Table 2. For such a system the splitting $\nu_E - \nu_{A2}$ should be positive according to Table 2, in full agreement with both theory and experiment, Table 1. On the other hand, $Co(ox)_3^{3-}$ has a considerable polar compression ($s/h > 1.29$) according to both theory and experiment.[34,35] It is thus not surprising that the TD-DFT method affords a negative splitting $\nu_E - \nu_{A2}$ for the $Co(ox)_3^{3-}$ complex in line with the predictions of Table 2.

The $Co(acac)_3$ complex is also interesting in having the largest azimuthal expansion ($\phi > 60°$) of $\phi = 69.3°$ and 67.3° according to respectively DFT and experiment,[34] Table 1. On the other hand $Co(ox)_3^{3-}$ is seen to suffer an azimuthal contraction ($\phi < 60°$) with $\phi = 56.2°$ (DFT) and 54.1° (expt[35]), respectively. One should thus expect the signs of R(E) and $R(A_2)$ to be respectively negative and positive for $Co(acac)_3$ according to Table 2. However, both experiment and TD-DFT theory find the signs of R(E) and $R(A_2)$ to be respectively positive and negative, Table 1. On the other hand, the calculated signs for R(E) and $R(A_2)$ in $Co(ox)_3^{3-}$ are in accord with the prediction of Table 2. We shall in a subsequent section discuss why $Co(acac)_3$ and $Co(ox)_3^{3-}$ have R(E) and $R(A_2)$ components of the same sign despite differences in their azimuthal parameters.

$M(NH_3)_6^{3+}$ as a Model for $M(X)_3^{3+}$ (M = Co, Rh; X = en, pn, tn). The rotatory strengths of the d−d transitions in tri-bidentate cobalt(III) complexes are determined by conformational (*lel* vs *ob*) as well as configurational (position of chelating atoms) factors. We shall now consider the simple system $Co(NH_3)_6^{3+}$ in which the conformational factors have been eliminated and examine to what degree this system can reproduce trends in the rotatory strengths for tri-bidentate diamine cobalt(III) complexes as a function of the polar and azimuthal distortions, Table 2.

We consider first $Co(NH_3)_6^{3+}$ of D_{3d} symmetry with the nitrogen atoms situated around cobalt in a perfectly octahedral arrangement and refer to this configuration as q^o. In a "σ-only" model we can describe the bonding in $Co(NH_3)_6^{3+}$

(50) Von Dreele, R. B.; Fay, R. C. J. *Am. Che. Soc.* **1971**, *93*, 4936.

Table 3. Metal d-Orbitals and Ligand σ-Orbitals Symmetrized According to the D_{3d} Point Group

symmetry combinations of σ-type ligand orbitals[a,b]	metal symmetry orbitals[c]
$L_\sigma(a_{1g}) = 1/\sqrt{6}\{\sigma_1 + \sigma_2 + \sigma_3 + \sigma_4 + \sigma_5 + \sigma_6\}$	$M_\pi(a_{1g}) = d_{z^2}$
$L_\sigma(a_{2u}) = 1/\sqrt{6}\{\sigma_1 + \sigma_2 + \sigma_3 - \sigma_4 - \sigma_5 - \sigma_6\}$	$M_\pi(e_{ga}) = \sqrt{\frac{2}{3}}d_{x^2-y^2} + \sqrt{\frac{1}{3}}d_{yz}$
$L_\sigma(e_{ga}) = 1/\sqrt{12}\{\sigma_1 + \sigma_2 - 2\sigma_3 + \sigma_4 - 2\sigma_5 + \sigma_6\}$	$M_\pi(e_{gb}) = \sqrt{\frac{1}{3}}d_{xz} + \sqrt{\frac{2}{3}}d_{xy}$
$L_\sigma(e_{gb}) = 1/2\{-\sigma_1 + \sigma_2 - \sigma_4 + \sigma_6\}$	$M_\sigma(e_{ga}) = \sqrt{\frac{1}{3}}d_{x^2-y^2} - \sqrt{\frac{2}{3}}d_{yz}$
$L_\sigma(e_{ua}) = 1/2\{\sigma_1 - \sigma_2 - \sigma_4 + \sigma_6\}$	$M_\sigma(e_{gb}) = \sqrt{\frac{2}{3}}d_{xz} - \sqrt{\frac{1}{3}}d_{xy}$
$L_\sigma(e_{ub}) = 1/\sqrt{12}\{\sigma_1 + \sigma_2 - 2\sigma_3 - \sigma_4 + 2\sigma_5 - \sigma_6\}$	

[a] Numbering scheme for ligands is shown in Scheme 6. [b] The symbols σ_i $\{i = 1,6\}$ represent the HOMOs of the six NH_3 ligands. Each HOMO is a σ-type lone pair pointing along the M−N bond vector. [c] The five d-orbitals

Table 4. Zero Order Many-Electron Determinantal Wave Functions for the States Involved in the d−d Transitions in the $Co(NH_3)_6^{3}$ Complex of D_{3d} Symmetry

state	wave function
$^1A_1$ ground state	$\lvert 1a_{1g}1\bar{a}_{1g}1e_{ga}1\bar{e}_{ga}1e_{gb}1\bar{e}_{gb}\rvert$
$^1A_{2g}$	$\frac{1}{\sqrt{2}}\{\lvert 1a_{1g}1\bar{a}_{1g}1e_{ga}1\bar{e}_{ga}1e_{gb}2\bar{e}_{ga}\rvert - \lvert a_{1g}\bar{a}_{1g}1e_{gb}1\bar{e}_{gb}1e_{ga}2\bar{e}_{gb}\rvert\}$
$^1E_{ga}$	$\frac{1}{2}\lvert a_{1g}\bar{a}_{1g}1e_{ga}1\bar{e}_{ga}1e_{gb}2\bar{e}_{gb}\rvert - \frac{1}{2}\lvert a_{1g}\bar{a}_{1g}1e_{ga}1\bar{e}_{ga}1e_{gb}2\bar{e}_{ga}\rvert - \frac{1}{\sqrt{2}}\lvert 1e_{ga}1\bar{e}_{ga}1e_{gb}1\bar{e}_{gb}1\bar{a}_{1g}2e_{ga}\rvert$
$^1E_{gb}$	$\frac{1}{2}\lvert a_{1g}\bar{a}_{1g}1e_{ga}1\bar{e}_{ga}1e_{gb}2\bar{e}_{ga}\rvert + \frac{1}{2}\lvert a_{1g}\bar{a}_{1g}1e_{gb}1\bar{e}_{gb}1e_{ga}2\bar{e}_{gb}\rvert - \frac{1}{\sqrt{2}}\lvert 1e_{ga}1\bar{e}_{ga}1e_{gb}1\bar{e}_{gb}1\bar{a}_{1g}2e_{gb}\rvert$

as involving the six occupied "σ_{NH_3}" lone pairs on the NH_3 ligands as well as the five d-orbitals on the metal atom, see Scheme 6. The corresponding orbital level diagram is shown in Scheme 7. Here the HOMOs involve the three degenerate nonbonding d-orbitals made up of the $M_\pi(a_{1g})$, $M_\pi(e_{ga})$, and $M_\pi(e_{gb})$ d-orbitals, Table 3, and designated, respectively, $1a_{1g}$, $1e_{ga}$, and $1e_{gb}$, Scheme 7. The two LUMOs on the other hand consist of $M_\sigma(e_{ga})$ and $M_\sigma(e_{gb})$ destabilized by out-of-phase interactions with the ligand combinations $L_\sigma(e_{ga})$ and $L_\sigma(e_{gb})$, Table 3. The two LUMOs are designated, respectively, Scheme 7.

The d−d excitations under consideration involve transitions from the $^1A_{1g}$ ground state to the excited states, Scheme 2. The zero order many-electron wave functions for the three states are given as a reference in Table 4. The rotatory strengths for the two d−d transitions are given as

$$R(A_2) = \mathrm{Im}\langle\Psi(^1A_{2g})|\vec{P}|\Psi(^1A_{1g})\rangle\langle\Psi(^1A_{2g})|\vec{M}|\Psi(^1A_{1g})\rangle \quad (1)$$

and

$$R(E) = \sum_d^{a,b}\mathrm{Im}\langle\Psi(^1E_{gd})|\vec{P}|\Psi(^1A_{1g})\rangle\langle\Psi(^1E_{gd})|\vec{M}|\Psi(^1A_{1g})\rangle \quad (2)$$

where

$$\vec{P} = \vec{r} \quad \text{and} \quad \vec{M} = -\frac{i}{2}\hbar(\vec{r} \times \vec{\nabla}) \quad (3)$$

It is readily shown that the matrix element involving the magnetic moment $\vec{M}$ is nonzero as all components of the $\vec{M}$ operator have even symmetry. On the other hand, the matrix elements involving the dipole operator $\vec{P}$ are seen to be zero since $\vec{r}$ is odd whereas the products between the ground state and excited state functions are even. We calculate in accordance with these considerations that $R(E)$ and $R(A_2)$ for conformation $q°$ must be zero, Table 4.

A polar elongation ($s/h < 1.22$) or compression ($s/h > 1.22$) does not change the D_{3d} symmetry of the complex since the polar coordinate change is associated with a normal mode of a_{1g} symmetry. The two components $R(E)$ and $R(A_2)$ will as a consequence remain zero, Table 4. On the other hand, a polar distortion will split the degeneracy of the HOMOs in Scheme 7. The sign of this splitting is not easy to predict by qualitative considerations. We find from our calculations that $\epsilon(1a_{1g}) > \epsilon(1e_g)$ for $s/h > 1.22$ and $\epsilon(1a_{1g}) < \epsilon(1e_g)$ for $s/h < 1.22$. It follows from Table 4 that only $1e_g$ (but not $1a_{1g}$) participates in the $^1A_{1g} \rightarrow {}^1A_{2g}$ transition whereas both $1e_g$ and $1a_{1g}$ contribute to the $^1A_{1g} \rightarrow {}^1E_g$ transition. It is thus understandable that $\nu_E - \nu_{A2} < 0$ for $s/h > 1.22$ and positive for for $s/h < 1.22$, Tables2 and 5.

The azimuthal contraction ($\phi < 60°$) or expansion ($\phi > 60°$) is associated with a normal mode of a_{1u} symmetry. Such a distortion reduces the overall symmetry of the complex to D_3. We shall in the following consider $\Delta\phi$ displacements away from the reference $q°$ conformation, where a positive value of $\Delta\phi$ corresponds to an expansion ($\phi > 60°$) whereas a negative value of $\Delta\phi$ represents a contraction ($\phi < 60°$).

Table 5. Circular Dichroism of Hypothetical[a] Λ-M$(NH_3)_6^{3+}$ (M = Co, Rh) Complex in the Gas Phase for Some Values of *s*/*h* and Φ Determined from Various Parents

		R (10^{-40} cgs)					
parent compound	band	model	real complex	ν (10^3 cm^{-1})	$\nu_E - \nu_{A2}$ (10^3 cm^{-1})	*s*/*h*	Φ (deg)
Λ-Co$(en)_3^{3+}$ $(lel)^3$	E	+32.8	28.9	27.122	−0.146	1.27	53.7
	A_2	−31.8	−25.0	27.268			
Λ-Co$(en)_3^{3+}$ $(ob)^3$	E	+20.7	17.5	27.222	−0.135	1.32	55.4
	A_2	−19.9	−12.2	27.357			
Λ-Rh$(en)_3^{3+}$ $(lel)^3$	E	+45.6	40.7	33.204	−0.477	1.37	52.1
	A_2	−49.6	−43.4	33.681			
Λ-Rh$(en)_3^{3+}$ $(ob)^3$	E	+34.5	36.5	33.273	−0.270	1.41	53.3
	A_2	−37.0	−29.9	33.543			
Λ-Co$(pn)_3^{3+}$ $(lel)^3$	E	+21.3	17.2	27.169	−0.286	1.27	52.1
	A_2	−21.2	−14.3	27.455			
Λ-Co$(pn)_3^{3+}$ $(ob)^3$	E	+8.7	11.6	27.289	−0.460	1.37	55.2
	A_2	−9.1	−2.0	27.749			
Λ-Rh$(pn)_3^{3+}$ $(lel)^3$	E	+49.2	34.2	33.414	−0.464	1.38	51.4
	A_2	−53.5	−32.4	33.877			
Λ-Rh$(pn)_3^{3+}$ (ob)	E	+32.8	37.2	33.535	−0.309	1.42	52.9
	A_2	−36.4	−23.5	33.844			
Λ-Co$(tn)_3^{3+}$ (lel)	E	−1.4	−10.3	25.262	−0.718	1.22	61.5
	A_2	1.4	8.2	25.980			
Λ-Co$(tn)_3^{3+}$ (ob)	E	+9.1	10.0	26.497	+0.194	1.25	59.6
	A_2	−8.7	−3.4	26.303			

[a] The different geometries of these model complexes are obtained from the transition metal complexes of Table 1 by changing each carbon chain by two H atoms.

We can write the wave function for the ground state and the first two excited singlet states at $q^\circ + \Delta\phi$ to first order in $\Delta\phi$ as

$$\Psi(^1A_1)_{(q^\circ+\Delta\phi)} = \Psi(^1A_{1g})_{q^\circ} + \frac{\Delta\phi\langle ^1A_{1g}|\partial\hat{H}/\partial\phi|^1A_{1u}\rangle_{q^\circ}}{E(^1A_{1u})_{q^\circ} - E(^1A_{1g})_{q^\circ}}\Psi(^1A_{1u})_{q^\circ} \quad (4a)$$

$$\Psi(^1A_2)_{(q^\circ+\Delta\phi)} = \Psi(^1A_{2g})_{q^\circ} + \frac{\Delta\phi\langle ^1A_{2g}|\partial\hat{H}/\partial\phi|^1A_{2u}\rangle_{q^\circ}}{E(^1A_{2u})_{q^\circ} - E(^1A_{2g})_{q^\circ}}\Psi(^1A_{2u})_{q^\circ} \quad (4b)$$

$$\Psi(^1E)_{(q^\circ+\Delta\phi)} = \Psi(^1E_g)_{q^\circ} + \frac{\Delta\phi\langle ^1E_g|\partial\hat{H}/\partial\phi|^1E_u\rangle_{q^\circ}}{E(^1E_u)_{q^\circ} - E(^1E_g)_{q^\circ}}\Psi(^1E_u)_{q^\circ} \quad (4c)$$

Here $^1A_{1g}$ is the ground state at q°, and $^1A_{2g}$ and ^1E_g are the two first singlet excited states from the d−d transitions at q°, Scheme 2, whereas $^1A_{1u}$, $^1A_{2u}$, and ^1E_u are excited states due to "charge transfer" transitions from the $L_\sigma(e_u)$ ligand orbitals, Table 3, to the $2e_g$ LUMO orbitals at q°, Scheme 7. It follows from eq 4 that an azimuthal distortion will add a fraction of "odd charge transfer" character to the wave functions for the states involved in the d−d transitions at $q^\circ + \Delta q$.

Thus, to first order in $\Delta\phi$ the nonzero part of the rotatory strengths for the two d−d transitions at $q^\circ + \Delta q$ becomes

$$R(A_2) = \mathrm{Im}\frac{\Delta\phi\langle ^1E_g|\partial\hat{H}/\partial\phi|^1E_u\rangle_{q^\circ}\langle ^1A_{1g}|\vec{P}|^1E_u\rangle_{q^\circ}}{E(^1E_u)_{q^\circ} - E(^1E_g)_{q^\circ}}\langle ^1A_{2g}|\vec{M}|^1A_{1g}\rangle_{q^\circ} \quad (5a)$$

and

$$R(E) = \sum_d^{a,b}\mathrm{Im}\frac{\Delta\phi\langle ^1E_{gd}|\partial\hat{H}/\partial\phi|^1E_{ud}\rangle_{q^\circ}\langle ^1E_{gd}|\vec{M}|^1E_{ud}\rangle_{q^\circ}}{E(^1E_{ud})_{q^\circ} - E(^1E_{gd})_{q^\circ}}\langle ^1E_{gd}|\vec{l}|^1A_{1g}\rangle_{q^\circ} \quad (5b)$$

It follows from the above expressions that both $R(A_2)$ and $R(E)$ will change sign in going from an azimuthal contraction ($\Delta\phi < 0$) to an azimuthal expansion ($\Delta\phi > 0$), in accordance with the predictions in Table 2.

Table 5 displays results from model calculations on M$(NH_3)_6^{3+}$ (M = Co, Rh) where the hexamine structures were generated by replacing the carbon chain in M$(X)_3^{3+}$ (M = Co, Rh; X = en, pn, tn) with two N−H bonds. Thus, the calculated rotatory strength for a hexamine complex derived from M$(X)_3^{3+}$ should afford a good estimate of the configurational (position of chelating atoms) contributions to $R(E)$ or $R(A/A_2)$ in M$(X)_3^{3+}$. It follows from Table 5 that the difference $|R(\text{model}) - R(\text{real complex})|$ in most cases amounts to 25% or less of $|R(\text{real complex})|$. Thus, we conclude that, for d−d transitions, the configurational contribution is the dominant factor in determining the rotatory strength for M(diamine)$_3^{3+}$ complexes. It is interesting to note that the reduction in $|R|$ in going from the $(lel)^3$ to the $(ob)^3$ conformation, Scheme 5, in many cases is well reproduced by the M$(NH_3)_6^{3+}$ model, Table 5.

A More Detailed Analysis of M$(NH_3)_6^{3+}$ and M$(X)_3^{3+}$ (M = Co, Rh; X = en, pn, tn). The analysis provided in eqs 1−5 has been rather formal and based on many-electron wave functions for the ground and excited states. However, the actual calculations discussed here are based on TD-DFT. This theory allows us in a rigorous way[13,14,40] to express the rotatory strength in terms of occupied and virtual ground state (Kohn−Sham) orbitals[13] that are solutions to the (Kohn−Sham) one-electron equation:[13]

$$h_{KS}(1)\psi_1(1) = \epsilon_i\psi_1(1) \quad (6)$$

In practice only approximate expresions are known for $h_{KS}(1)$. The calculated values for R are as a consequence not exact. For the d−d transitions we find for $M(NH_3)_6^{3+}$ of Table 5 that 95% of $R(A_2)$ and $R(E)$ can be expressed in terms of the HOMOs and LUMOs of Scheme 7. This would also be the case if we substituted the zero-order many-electron wave function of Table 4 into the expressions for the rotatory strengths of eqs 1 and 2. Starting at configuration $q°$ of $M(NH_3)_6^{3+}$ with D_{3d} symmetry we find for the part of the rotatory strengths that is expressed in terms of the HOMOs and LUMOs

$$R(A_{2g}) \propto \langle 1e_{ga}|\vec{P}|2e_{gb}\rangle\langle 2e_{gb}|\vec{M}|1e_{ga}\rangle \quad (7a)$$

$$R(E) \propto \langle 1e_{ga}|\vec{P}|2e_{ga}\rangle\langle 2e_{ga}|\vec{M}|1e_{ga}\rangle \quad (7b)$$

Symmetry considerations again reveal that the two matrix elements in eq 7 involving $\vec{P}$ are zero since $\vec{P}$ is odd whereas the HOMOs and LUMOs are even functions. Going next to configuration $q° + \Delta\phi$ of D_3 symmetry allows even metal orbitals to mix with odd ligand combinations. Of special importance for this discussion is the fact that the odd $L_\sigma(e_{uc})$ ($c = a, b$) ligand combinations will overlap with the even metal orbitals $M_\pi(_c)$ ($c = a, b$), Scheme 8. We find thus at $q° + \Delta\phi$ the two HOMOs have the form

$$1e_c = M_\pi(e_{gc}) + \Delta\phi C_{mix} L_\sigma(e_{uc})_{(q° + \Delta\phi)} \quad (c = a, b) \quad (8a)$$

whereas the LUMO still can be written as

$$2e_c = M_\sigma(e_{gc}) - C_{L_s} L_\sigma(e_{gc})_{(q° + \Delta\phi)} \quad (c = a, b) \quad (8b)$$

It should be noted that the index $q° + \Delta\phi$ attached to the ligand orbitals in eq 8 indicates that the ligand combination coefficients defined in Table 3 still are the same but that the individual ligands have been displaced by $\Delta\phi$, see also Scheme 8. It follows from eq 8a that the HOMOs have

Scheme 8 The Generation of an Overlap between the Odd Ligand Combination $L_\sigma(e_{ua})$ and the Even $M_\pi(e_{ga})$ Metal d-orbital Due to an Azimuthal Distortion of the Octahedron

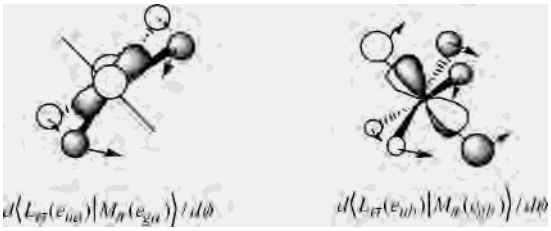

borrowed some odd ligand character by the azimuthal distortion $\Delta\phi$ where the mixing coefficient in eq 8a can be expressed in by ordinary perturbation theory[51−56] as

$$C_{mix} = \frac{\langle L_\sigma(e_{uc})_{(q°)}|dh_{KS}/d\phi|M_\pi(e_{gc})\rangle - \langle L_\sigma(e_{uc})_{(q°+\Delta\phi)}|M_\pi(e_{gc})\rangle\epsilon(M_\pi(e_{gc}))}{\epsilon(M_\pi(e_{gc})) - \epsilon(L_\sigma(e_{uc})_{q°})} \quad (9)$$

Thus, mixing is mediated by a change in the (Kohn−Sham) one-electron operator $dh_{KS}/d\phi$ as well as the emergence of an overlap between the even metal orbital and the odd ligand combination, Scheme 8. Keeping only leading terms affords finally the following relations:

$$R(A_2) \propto \Delta\phi C_{mix}\langle L_\sigma(e_{ua})_{(q°+\Delta\phi)}|\vec{P}|L_\sigma(e_{gb})_{(q°)}\rangle\langle 2e_{gb}|\vec{M}|1e_{ga}\rangle \quad (10a)$$

$$R(E) \propto \Delta\phi C_{mix}\langle L_\sigma(e_{ua})_{(q°+\Delta\phi)}|\vec{P}|L_\sigma(e_{ga})_{(q°)}\rangle\langle 2e_{gb}|\vec{M}|1e_{ga}\rangle \quad (10b)$$

In TD-DFT we can in general express[40−42] rotatory strengths corresponding to the transition $0 \rightarrow \lambda$ as

$$R(0\rightarrow\lambda) = \sum_{\mu,\nu} A^\lambda_{\mu,\nu}\langle\chi_\mu|\vec{P}|\chi_\nu\rangle \sum_{\mu,\nu} B^\lambda_{\mu,\nu}\langle\chi_\mu|\vec{M}|\chi_\nu\rangle \quad (11)$$

where $A^\lambda_{\mu,\nu}$ and $B^\lambda_{\mu,\nu}$ are matrices associated with the transition $0 \rightarrow \lambda$ and spanned by the basis set χ_μ,χ_ν. The matrices A and B are further determined by solving a set of coupled differential (RPA) equations.[40−42] In the ADF program it is further possible as basis set to use symmetrized linear combinations of ligand orbitals (occupied and virtual) as well as metal orbitals. It is thus possible from inspection to see what combinations of $\{\chi_\mu,\chi_\nu\}$ will contribute to $R(0 \rightarrow \lambda)$. We find for $M(NH_3)_6^{3+}$, Table 5, that 90% of the transition moment involving $\vec{P}$ originates from the coupling between $L_\sigma(e_{uc})$ and $L_\sigma(e_{gc})$ as discussed above in eq 7 whereas the magnetic moment involving $\vec{M}$ primarily comes from the coupling between $M_\pi(e_{gc})$ and $M_\sigma(e_{gc})$, Table 3.

In $M(X)_3^{3+}$ we have again a set of six σ-type lone-pair orbitals $\{\sigma_i; i = 1, 6\}$ each attached to a nitrogen atom. The only (minor) difference from $M(NH_3)_6^{3+}$ is that the σ-type orbitals are teetered together in pairs. It is thus not surprising that the electron structure of $M(X)_3^{3+}$ to a first approximation can be described by the symmetry orbitals given in Table 3. The only qualification is that $M(X)_3^{3+}$ even at the configuration $q°$ has D_3 symmetry due to the carbon chains. Also, $M(X)_3^{3+}$ will have orbitals (of lower energy) describing these chains. Nevertheless, a full calculation on $M(X)_3^{3+}$ revealed through an analysis based on eq 11 that 90% of the transition moment involving $\vec{P}$ originates from the coupling between $L_\sigma(e_{uc})$ and $L_\sigma(e_{gc})$ as discussed above in eq 7 whereas the magnetic moment involving $\vec{M}$ primarily comes from the coupling between $M_\pi(e_{gc})$ and $M_\sigma(e_{gc})$, Table 3. It is important to note that $M(X)_3^{3+}$ exhibit optical activity even at the configuration $q°$ due to the electrostatic potential of the carbon chains connecting the chelating nitrogen atoms. This potental is again able to mix the odd ligand combination $L_\sigma(e_{uc})$ into the HOMO.

An analysis of the results for $M(X)_3^{3+}$ (X = en, pn, tn) based on eq 11 reveals that matrix elements $\langle\chi_\mu|\vec{P}|\chi_\nu\rangle$ between odd (e.g. $(n + 1)$p) and even (e.g. nd) metal orbitals are responsible for less that 5% of the transition moment P,

(51) Mason, S. F.; Norman, B. J. *Chem. Commun.* **1965**, 48.
(52) Piper, T. S.; Karipides, A. *Mol. Phys.* **1962**, *5*, 475.
(53) Shinada, M. *J. Phys. Soc. Jpn.* **1964**, *19*, 1607.
(54) Mason, S. F. *J. Chem. Soc. A* **1971**, 667.
(55) Iwata, M.; Nakatsu, K.; Saito, Y. *Acta Crystallogr., Sect. B* **1969**, *25*, 2562.
(56) Pople, A. A.; Krishnan, R.; Schlegel, H. B.; Binkley, J. S. *Int. J. Quantum Chem. Symp.* **1979**, *13*, 225.

although they should be the exclusive contributors according to crystal field theory.[3] Also minor (<5%) is the importance of matrix elements involving a metal orbital and a ligand orbital. Such terms have been considered major in qualitative molecular orbital theory.[5−7,9] In the dynamic theory by Mason and Seal[11] the important contribution to P comes from matrix elements between occupied and virtual ligand orbitals. However, our analysis finds that they are of little importance (<5%) for X = en, pn, tn. They might nevertheless contribute significantly in the case of other ligands as we shall show shortly.

A More Detailed Analysis of $Co(ox)_3^{3-}$ and $Co(acac)_3$. The electronic structure of these two complexes is somewhat more complicated than the amine systems in that we in addition to the σ-based ligand combinations $L_\sigma(e_{uc})$ and $L_\sigma(e_{gc})$ also have participation in the HOMOs and LUMOs from (even and odd) π-type ligand combinations made up of π_{CO} and π^*_{CO} orbitals. The even π-type combinations can mix into the HOMO already in a perfectly octahedral configuration whereas participation from an odd combination takes place via an azimuthal distortion in a way[5−7,57] similar to that involving $L_\sigma(e_{uc})$. The transition moment will as a consequence have contributions from couplings between (odd and even occupied) σ-orbitals, π-orbitals, or σ-orbitals and π-orbitals. We have in addition for $Co(acac)_3$ some coupling between occupied π_{CO} and π^*_{CO} orbitals.The many different contributions (with different signs) to the transition moments make it understandable why the signs for $R(E)$ and $R(A_2)$ do not follow the same pattern as the amine complexes with regard to azimuthal distortions.

4. Conclusions

The singlet transitions and their rotatory strengths have been studied in the d−d excitation region for a number of Co(III) and Rh(III) complexes by the TD-DFT method. The agreement with experiment is only qualitative and the calculated R values might differ by as much as a factor of 2 compared to experimental estimates. Other recent TD-DFT studies have found similar deviations for organic molecules.[58]

The studied complexes exhibit two main d−d excitations corresponding to the $^1A_1 \rightarrow {}^1A_2$ and $^1A_1 \rightarrow {}^1E$ transitions. It is explained from model calculations on $Co(NH_3)_6^{3+}$ and $Rh(NH_3)_6^{3+}$ how configurational distortions of the nitrogen atoms away from a perfect octahedron influence the d−d spectrum. Thus, a deformation of the octahedron along a C_3 axis (polar deformation) will split the energy degeneracy of the $^1A_2$ and ^1E excited states with $^1A_2$ being of highest energy for an elongation and of lowest energy for a compression. On the other hand, an azimuthal distortion (Scheme 4) will introduce optical activity with rotatory strengths for the two bonds of opposite signs. Further, $R(A_2)$ is positive for $\Delta\phi > 0$ and negative for $\Delta\phi < 0$. It is further shown that the tris-diamine complexes $M(X)_3^{3+}$ (M = Co, Rh; X = en, pn, tn) exhibit the same trends with respect to polar and azimuthal distortions. These trends were first noted by Stiefel and Brown[29] as well as Judkins and Royer.[30]

The d−d transitions in an octahedral complex are formally forbidden with a zero transition moment since both the HOMO and LUMO d-orbitals are even. This is not helped by the fact that the even σ-type ligand combination $L_\sigma(e_{gc})$ will mix with the d-orbital of the LUMO. However, an azimuthal distortion of the octahedron will allow the odd ligand combination $L_\sigma(e_{uc})$ to mix with the d-orbital of the HOMO. This mixing will contribute to nonzero transition moment $\langle L_\sigma(e_{uc})|\vec{P}|L_\sigma(e_{gc})\rangle$ as well as a rotatory strength where the magnetic moment comes from coupling between the d-orbitals. For $M(X)_3^{3+}$ (M = Co, Rh; X= en, pn, tn) the coupling between $L_\sigma(e_{gc})$ and $L_\sigma(e_{uc})$ accounts for 90% of the transition moments. On the other hand there is little coupling between (even and odd) metal orbitals (as suggested by crystal field theory); between (even and odd) ligand and metal orbitals (as suggested by ligand field theory and qualitative molecular orbital theory); or between (even and odd) occupied and virtual ligand orbitals (as implied in the dynamic theory by Mason *et al.*[11]).

The origin of optical activity in $Co(ox)_3^{3-}$ and $Co(acac)_3$ is slightly more complex. For these complexes one finds in addition to the coupling between $L_\sigma(e_{gc})$ and $L_\sigma(e_{uc})$ also coupling between (odd and even) π_{CO} and π^*_{CO} ligand combinations.

Acknowledgment. This work has received financial support from the National Science and Engineering Research Council of Canada (NSERC). One of us (F.E.J.) would like to acknowledge the financial support of CAPES (Brazilian Research Agency). T.Z. would like to thank the Canadian Government for a Canada Research Chair.

IC034997T

(57) Ballhausen, C. J. In *Molecular Electronic Structures of Transition Metal Complexes*; McGraw-Hill: New York, 1979; p 195.
(58) Diedrich, C.; Grimme, S. *J. Phys. Chem. A* **2003**, *107*, 2524